Monitoring Of The LANDSLIDE Phenomenon Using Wireless Sensor Networks

Saman Shoorabi Sani[1,*], Majid Baghaei-Nejad[2] ,Mona Kalate Arabi[3]
1- Faculty of Electrical and Computer Engineering, Hakim Sabzevari University, Sabzevar, Iran.
[*]Email: s1sani91@gmail.com(Corresponding author)
2- Faculty of Electrical and Computer Engineering, Hakim Sabzevari University, Sabzevar, Iran.
Email: mbnejad@hsu.ac.ir
3- Faculty of Electrical and Computer Engineering, Islamic Azad University of Neyshabur,
Science and Research Branch, Iran
Email: MONA.KALATEARABI.1387@GMAIL.COM

Received X X X Revised X X X Accepted X X X

ABSTRACT:
This paper presents a WSN-based method for monitoring the displacement in landslide susceptible slopes. In this method, an array of wireless transmitters installed on the target slope will broadcast regular signals, which will be received and interpreted by two synchronous receivers. The proposed system monitors the slope by measuring the phase difference between the two mentioned receivers before and after displacements, and shows promising reliability and accuracy for monitoring the status of landslide susceptible mountainous terrains. This approach did not have any field trial, but its results and accuracy has been evaluated through a series of comprehensive simulations performed for an array of six transmitter (Tx) and two receivers (Rx).

KEYWORDS: Real-time Landslide Monitoring, Wireless Sensor Network

1. INTRODUCTION

There have been many efforts to predict and control natural disasters such as landslides. The most important factor of distinction between these methods is the extent of their area of interest or AOI. Some methods are suitable for regions smaller then several hundred square meters; these methods are usually based on laser beams and WSN-based transmitter-receiver systems [1-3]. The second group includes those methods that process SAR[1] produced images to monitor a vast AOI [4-6]. The third group consists of those methods that measure geological and hydrological parameters of the target slope to monitor and predict the possibility of landslide [7]. For example, sensors such as pressure transducers, geophones, moisture meters etc. could use a wireless sensor network to transmit valuable data about an AOI; data that can later be processed to estimate its features or hazards. The mentioned methods are the most popular approaches for predicting or monitoring landslides, but, as always, each approach has its own advantages and drawbacks. For instance, methods of first group have a high level of power consumption and cannot be safely implemented in residential areas; methods of second group are very time consuming and their accuracy is subject to effects of climatic conditions; methods of third group require a multitude of expensive equipment, which can be a major issue for large scale projects [8-11].More details and examples of the similar and innovative methods and applications have been stated in [12-17].

2. GEOMETRICAL PRINCIPLES AND SIGNAL PROCESSING

Considering the financial and technical limitations of methods mentioned in introduction, objective of this paper is to present a novel simulation-based method for monitoring the slopes susceptible to landslide. This new method, which is based on simulation via MATLAB software and is coded by C#, can detect, monitor and report small displacements in the target slope. The program developed for this method is equipped with a graphical user interface (GUI) that simplifies the data entry process and ensures the clarity of produced results.Theoretical and mathematical principles of the proposed method are explained below.

In this landslide detection technique, an array of transmitters (TX) will be installed on the target area and will send regular signals to two synchronous wireless receivers. This system measures the changes in phase difference (caused by displacement of transmitters) and estimate the real-time status of the target slope with a tenth of a millimeter accuracy. The

[1] Synthetic Aperture Radar

mentioned synchronous receivers will be installed in a location safely away from the target area and will demodulate the received signals independently but with considering the correlations. Here, the main problem will be to detect and counter an "ambiguous state", in which displacement may occur without any detectable change in phase difference. So far, the proposed approach has only been tested in simulations and is yet to be implemented in a field trial.

As mentioned in introduction, monitoring the landslide-susceptible slopes has been the subject of extensive research and there are currently several methods that can be used for this purpose. But this study aims to use the concept of phase difference between two receivers to develop an inexpensive and low-noise method to detect and measure displacements. This monitoring system will measure the phase difference pertaining to the transmitter installed in the AOI[1] (which is the target slope) and the synchronized receiving nodes, which must be installed in a location slightly away from the AOI. An array of transmitters (TXs) will be configured to repeatedly and synchronously broadcast the string of (11111111) on a specific carrier frequency (4 GHz). The receiver nodes will be installed in a location close to each other but away from the slope and will demodulate the signals independently but with a shared synchronous oscillator. The system will be able to use IEEE 802.11n network protocol and its related equipment to quickly detect the displacements and deformations in an area of about 2500 square-meter. Collected data can be sent to a secondary control center for further processing. This technique is resources-efficient since it enables several arrays of transmitters and antennas to share a single data transmission circuit. In the rest of this paper, we will first assess a system composed of a single TX and describe that how a phase shift can be interpreted into a displacement value; then we will extent the theory for a system composed of an array of TXs. Next, we will discuss the ambiguous state (path) and its mathematical definition and equations. We will then present the block diagram of the receivers and will describe the signals of transmitter and receiver at each step, from the start of transmission until the end of detection. Finally, a series of 3-D simulations will be performed to demonstrate the process of work and estimate its errors.

2.1. Wireless transmitter - receiver model

Figure 1 shows an overview of the proposed landslide detection system. Here, the AOI is a slope overlooking a residential zone. An array of TXs (named T1 to T6) is installed on the AOI and is configured to send a certain data sequence to the receivers (during the training phase). These two synchronous receiver nodes (named R0 and R1) are installed closely to each other (with a certain and predefined spacing) but at a distance away from the AOI.

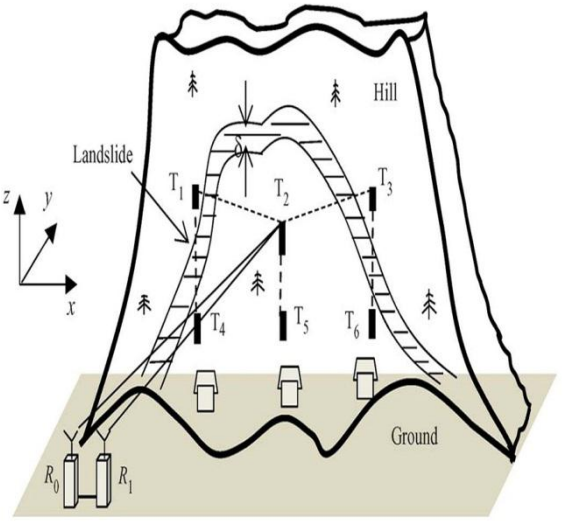

Fig. 1 Global view of the innovative system for monitoring of the landslide phenomenon

2.2. Calculation of displacement in a single-TX system

Figure 2 shows a 3D view of the model of the proposed landslide detection system. $T(x_0,y_0,z_0)$ is the location of transmitter on AOI; the first receiver (R0) is located at (0, 0, 0) and the second one (R1) is located at (a, 0, 0). T' is the location of the point T after the displacement. δ is the magnitude of displacement or deformation and points p(x0,y0,0) and p' (x1,y1,0) are the projections of T and T' on the X-Y plane. Deviation lines (r0,r1) and (r_0', r_1') are the distances of R0 and R1 from T and T'.

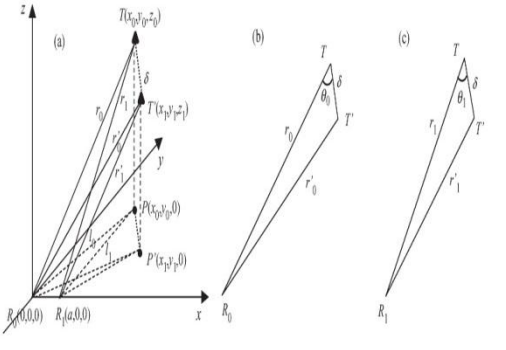

Fig. 2 status of point T and its post-displacement equivalent T'

[1] Area Of Interest

We have: $r_0 = \sqrt{x_0^2 + y_0^2 + z_0^2}$ and $r1 = \sqrt{(x_0 - a)^2 + y_0^2 + z_0^2}$.

θ_0 and θ_1 are the angles between the lines $R_1 - T$, $T - T'$, $R_0 - T$ and T-T'. Location of R_0 and R_1 and TXs should be recorded in the course of installation so that parameters a, Z_0, Y_0, X_0 could be determined. Slope vector at point T can be obtained by the following equation (using numerical analysis techniques):

$$\vec{M} = (x_1 - x_0)\hat{x} + (y_1 - y_0)\hat{y} + (z_1 - z_0)\hat{z} \quad (1)$$

The scalar value of this vector is:

$$M_{Th} = (z_1 - z_0) / \sqrt{(x_1 - x_0)^2 + (y_1 - y_0)^2} \quad (2)$$

Without knowing T' (x_1,y_1,z_1), to obtain θ_0 and θ_1 we need to calculate the phase difference φ_D in terms of distance D=r_0-r_1. Since $D' = r_0' - r_1'$, without knowing the location of T', phase difference φ_D' can only be calculated via the receiver nodes.

According to triangles $T - T' - R_0$, $T - T' - R_1$ we can argue that:

$$\vec{r}_0^{\,2} + \vec{\delta}^2 - 2r_0 \cdot \vec{\delta} \cdot \cos\theta_0 = \vec{r}_0'^{\,2}$$
$$\vec{r}_1^{\,2} + \vec{\delta}^2 - 2r_1 \cdot \vec{\delta} \cdot \cos\theta_1 = \vec{r}_1'^{\,2} \quad (3)$$

Therefore:

$$r_0' \approx r_0 - \vec{\delta} \cdot \cos\theta_0$$
$$r_1' \approx r_1 - \vec{\delta} \cdot \cos\theta_1 \quad (4)$$

where θ_0, θ_1, r_0 and r_1 are parameters measured during installation. Having obtained D=r_0-r_1 and $D' = r_0' - r_1'$ we have:

$$\vec{\delta} = \frac{D - D'}{\cos\theta_0 - \cos\theta_1} \quad (5)$$

In equation (3), D' is unknown, but it can be calculated with the help of measured phase φ_D'

$$D' = \lambda \cdot \varphi_D' / 360 \quad (6)$$

In the above equation, λ is the wavelength of carrier frequency. It should be noted that φ_D' is a (complex or irrational) number and $0 < \varphi_D' < 360$. Therefore, equation (4) only provides the fractional part of D'.

For $\delta < \lambda$, the value of $D - D'$ is the fractional part of λ. The integral part of D' can be obtained from D. so having $D = r_0 - r_1 = N_D.\lambda + \Delta D$, r_1, r_0 and knowing that $\Delta D = D - N_D \cdot \lambda, N_D = mod[D, \lambda]$, the correct value of D' can be calculated by the $D' = N_D \cdot \lambda + \Delta D'$. Since $D - D'$ is a fraction of λ and D– D′ = $\Delta D - \Delta D'$, we have:

$$\delta = \frac{\Delta D - \Delta D'}{\cos\theta_0 - \cos\theta_1} \quad (7\text{-}1)$$

As equation (7-1) clearly shows, the main causes of error in measurement are θ_0 and θ_1, which both are dependent on the direction of displacement. Now assuming that $\theta_1' = \theta_1 + \varepsilon$, $\theta_0' = \theta_0 + \varepsilon$ where ε is a small error (deviation), δ' (due to ε) can be obtained through following equation:

$$\delta' = \frac{\Delta D - \Delta D'}{\cos(\theta_0 + \varepsilon) - \cos(\theta_1 + \varepsilon)}$$
$$\approx \frac{\Delta D - \Delta D'}{\cos\theta_0 - \cos\theta_1 - \varepsilon \cdot (\sin\theta_0 - \sin\theta_1)} \quad (7\text{-}2)$$

Displacement error due to ε will be:

$$\Delta\delta = \delta' - \delta$$
$$\approx \varepsilon \cdot (\Delta D - \Delta D') \cdot \frac{\sin\theta_0 - \sin\theta_1}{(\cos\theta_0 - \cos\theta_1)^2}$$
$$\frac{\Delta\delta}{\delta} \approx \varepsilon \cdot \frac{\sin\theta_0 - \sin\theta_1}{\cos\theta_0 - \cos\theta_1} \quad (8)$$

3. A SYSTEM WITH ARRAYS OF TXS

The explained single-TX system can be easily extended to a two-dimensional system with arrays of TXs and be used to monitor a wide area for displacements. Figure 1 shows an instance of a (2 × 3) TX array.

Each TX of the array is configured to broadcast its signal sequence on a regular basis. Each TX can have its own slope vector. TXs of an array could share a single transmission circuit via a multiplexer so that the cost of hardware and equipment could be reduced. Two synchronized receivers demodulate the broadcasted signals, identify the source TX and determine and calculate the displacement corresponding to the source.

4. AMBIGUOUS STATE (PATH)

An ambiguous state (path) is a state in which after displacement the phase difference between the

receivers remains unchanged. This state occurs when $r_0' - r_1'$ equals $r_0 - r_1$. According to the procedure described in the previous section, when displacement is such that $T'(x_1, y_1, z_1)$ results in an ambiguous state, method fails to detect the displacement.

As Figure 3 shows, considering the curved lines r_0 and r_1, the point T can be located on the circle resulted from intersection of two spheres with radiuses r_0 and r_1. Therefore, $T(x_0, y_0, z_0)$ satisfies the equation $(x_0 - a)^2 + y_0^2 + z_0^2 = r_1^2, x_0^2 + y_0^2 + z_0^2 = r_0^2$. The circle resulted from the intersection of the two spheres is located on Y-Z plane and assuming that x=x0, we have:

$$x_0 = (a^2 + r_0^2 - r_1^2)/2a = c/2a$$
$$c = a^2 + r_0^2 - r_1^2$$
$$y_0^2 + z_0^2 = r_0^2 - c^2/(4a^2) \quad (9)$$

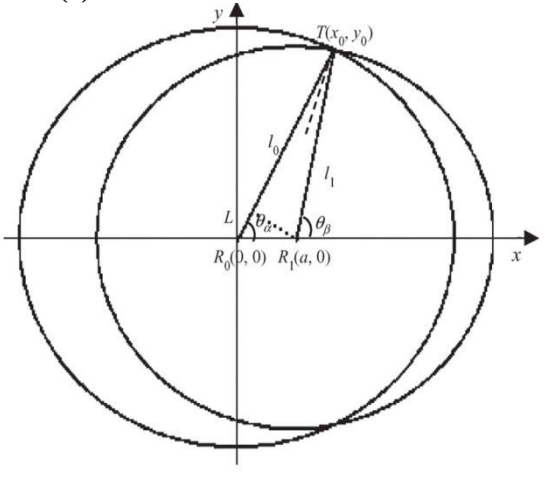

Fig. 3 Geometrical status of ambiguous state

Center of circle is located at $(c/2a, 0, 0)$ and its radius is $\sqrt{r_0^2 - c^2/(4a^2)}$. Ambiguous state happens when displacement or movement of slope is in a way that r_0 and r_1 both change by the same δ. Therefore, $\delta > o$, $r_1' = r_1 - \delta$, $r_0' = r_0 - \delta$ (because of gravity), and assuming that $C' = C - 2(r_0 - r_1)\delta$, intersection of two new spheres (with radiuses of r_1', r_0') create a new circle with new $x = x'$ and new radius:

$$x_1^2 + y_1^2 + z_1^2 = r_0'^2$$
$$(x_1 - a)^2 + y_1^2 + z_1^2 = r_1'^2$$
$$\Rightarrow x_1 = [c - 2(r_0 - r_1)\delta]/2a$$
$$= c'/2a$$
$$y_1^2 + z_1^2 = (r_0 - \delta)^2 - \frac{c'^2}{4a^2} \quad (10)$$

T' is the intersection of the slope with this new circle. The center of this circle is located at ($c'/2a, 0, 0$) and its radius is $\sqrt{(r_0 - \delta)^2 - (c'^2/4a^2)}$ which is approximately equal to $r_0 - (c^2/8a^2 r_0) - [1 - c(r_0 - r_1)/(2a^2 r_0)]\delta$. In this three-dimensional system, the ambiguous path is represented by the locus of T' created by variation of values r_1', r_0'. It would be very hard to obtain a three-dimensional equation for this ambiguous path. So we solve it in two dimensions, and then obtain the value of Z from the slope of ambiguous path $m_{ah} = (z_1 - z_0)/\sqrt{(x_1 - x_0)^2 + (y_1 - y_0)^2}$. In X-Y plane, T can be obtained from the intersection of two circles created by the intersection of two spheres with $z_0 = 0$ and radius of L_0 and L_1.

We have:

$$L_0 = r_0 \cos\theta_\alpha$$
$$L_1 = r_1 \cos\theta_B$$
$$\theta_\alpha = tg^{-1}(y_0/x_0)$$
$$\theta_\beta = tg^{-1}[(y_0/(x_0 - a)] \quad (11)$$

where θ_B, θ_α are the angles between R_1, R_0 and point T. $[L = L_0 - L_1]$ is the difference in the magnitude of deviation. As shown in figure 3, these two circles can be assumed as the projection of a 3D space on a 2D plane. Assuming that $z = 0$, equation (10) can be simplified for X-Y plane:

$$x = \frac{c - 2(l_0 - l_1)\delta}{2a}$$

$$y^2 = (l_0 - \delta)^2 - [\frac{c}{2a} - \frac{(l_0 - l_1)\delta}{a}]^2$$

$$y \approx l_0 - \frac{c^2}{8a^2 l_0} - [1 - \frac{c(l_0 - l_1)}{2a^2 l_0}]\delta$$

$$\approx l_0 - \frac{c^2}{8a^2 l_0} - \delta \quad (12)$$

By eliminating δ from x and y in the above equation, we will have:

$$y = l_0 - \frac{(a^2 + l_0^2 - l_1^2)^2}{8a^2 l_0} - \frac{a^2 + l_0^2 - l_1^2}{2(l_0 - l_1)} + \frac{a}{(l_0 - l_1)}x$$

$$= m_a x + K \quad (13)$$

where $m_a = a/(L_0 - L_1)$ is the slope of ambiguous path and

$$K = l_0 - (a^2 + l_0^2 - l_1^2)^2/(8a^2 l_0) - (a^2 + l_0^2 - l_1^2)/(2(l_0 - l_1)) \quad (14)$$

Equation (13) is the equation of ambiguous path in X-Y plane. Having T and $m_{ah,}$ the height of ambiguous path at point T' can be obtained from the following equation:

$$z = z_0 - m_{ah} \cdot \sqrt{(x_0 - x)^2 + (y_0 - y)^2} \quad (15)$$

Figure 4 shows the ambiguous path in the X-Y plane. As can be seen, TX and receivers are located at $T(40_m, 200_m)$ and $R_0(0,0)$ and $R_1(a,0)$ with $\alpha = 1$ to $\alpha = 5$. Figure (4-a) shows the state where L_1, L_0 are reduced by the same δ , and Figure (4-b) shows the path based on equation 13. In both cases, ambiguous path is expressed as a function of α (the distance between R_1 and R_0). For each x, the difference between the y in the path of Figure (4- a) and the y in the path of Figure (4–b) is shown in Figure (4-c).

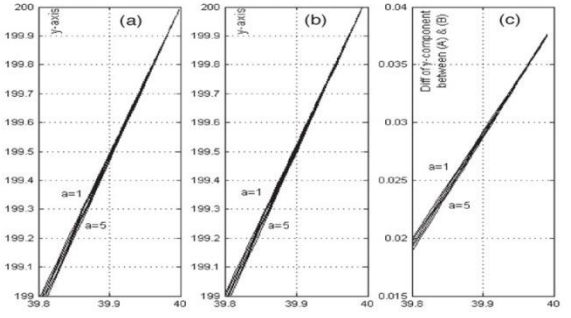

Fig. 4 The ambiguous path on X-Y plane (the error in y is expressed as a function of a)

Because of gravity, Z component of point TX decreases during the displacement. So it will be enough to check that whether the slope m_{Th} matches the slope m_{ah} (ambiguous path) on X-Y plane. If $m_a = m_T$ the detection technique fails only when $m_T = (x_1 - x_0)/(y_1 - y_0)$. Equation (7-1) can be used to calculate the deviation of ground in a single TX system. In case of an array of TXs, each TX will have its own slope and ambiguous path. In this case, location of the two receiver nodes must be designed in a way that none of the ambiguous paths match the displacement or deformation path.

5. BLOCK DIAGRAM AND SIGNAL ANALYSIS OF TRANSMITTER-RECEIVER SYSTEM

Figure 5 shows the block diagram of the proposed transmitter-receiver system with one TX and two receivers. A typical TX broadcasts a signal with a fixed carrier frequency. Carrier frequency (Fc) is different from frequency of receivers.

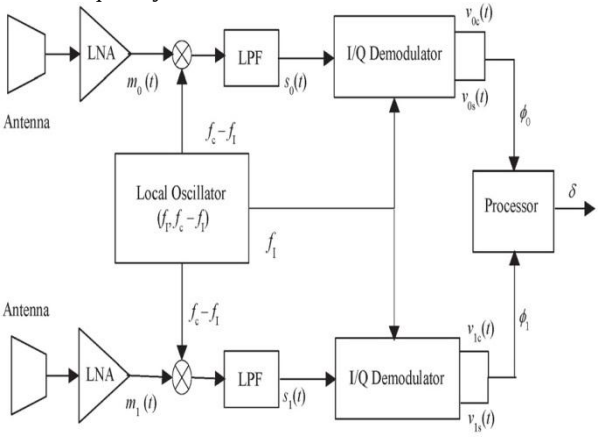

Fig. 5 Block diagram of the synchronous receiver system

The typically required efficiency is between -25ppm[1] and +25ppm (in the range frequency at which system is sustainable). So the maximum error of Fc between transmitter and receiver will be 50ppm. Assuming that carrier frequency of TX is $Fc + \Delta Fc$, the carrier frequency of receiver will be Fc with a maximum frequency difference of $\Delta F_c = 0.5 \times F_c / 10^4$. In Figure 5, a local oscillator is shared between two receiver nodes, which create two frequencies of F_I (Intermediate frequency band) and F_c - F_I. Amplified signals $m_1(t), m_0(t)$ are demodulated independently by a frequency of Fc-FI. These two signals are then passed through a low-pass filter to create $S_1(t), S_0(t)$. Two (I-Q) in-phase quadrature demodulators are used to generate base-band signals $v_1(t), v_0(t)$, which later will be used to generate the phase difference data pertaining

[1] Pulse per minute

to receiver nodes. Assuming that p(t) is the signal sent by TX and $p(t) = \cos[(w_c + \Delta w_c)t], 0 \le t \le T_p$, and T_p is the pulse period, the received signals $m_0(t)$,$m_1(t)$ will be in the following form:

$$m_0(t) = \cos[(w_c + \Delta w_c)(t - \tau_0)]$$
$$m_1(t) = \cos[(w_c + \Delta w_c)(t - \tau_1)] \quad (16)$$

where τ_1, τ_0 are the delays from TX to receivers R_1 and R_0. After multiplying $m_0(t)$ and $m_1(t)$ by the frequency F_c - F_i and passing them through the low-pass filter, we will have:

$$s_0(t) = \frac{1}{2}\cos[(\Delta w_c + w_i)t - (w_c + \Delta w_c)\tau_0]$$
$$s_1(t) = \frac{1}{2}\cos[(\Delta w_c + w_i)t - (w_c - \Delta w_c)\tau_1] \quad (17)$$

These two intermediate frequencies are sent to an I-Q demodulator, creating the base band signals $v_{1c}(t)$, $v_{1s}(t)$, $v_{0s}(t)$, $v_{0c}(t)$ shown below:

$$v_{0c}(t) = \frac{1}{4}\cos[\Delta w_c t - (w_c + \Delta w_c)\tau_0]$$
$$v_{0s}(t) = -\frac{1}{4}\sin[\Delta w_c t - (w_c + \Delta w_c)\tau_0]$$
$$v_{1c}(t) = \frac{1}{4}\cos[\Delta w_c t - (w_c + \Delta w_c)\tau_1]$$
$$v_{1s}(t) = -\frac{1}{4}\sin[\Delta w_c t - (w_c + \Delta w_c)\tau_1] \quad (18)$$

The phase difference is:

$$\varphi_D(t) = \varphi_0 - \varphi_1$$
$$= \tan^{-1}[\frac{v_{0s}(t)}{v_{0c}(t)}] - \tan^{-1}[\frac{v_{1s}(t)}{v_{1c}(t)}]$$
$$= (\mathrm{w_c} + \Delta\,\mathrm{w_c})(\tau_0 - \tau_1) \quad (19)$$

Phase φ_D is obtained in the course of installation (during the training phase). After the installation, phase φ_D' will be measured and will be used to calculate $\Delta D' = r_0' - r_1'$. When $\Delta D = r_0 - r_1$, the base displacement (δ) can be obtained from the equation (7-1).Since $\Delta F_c / F_c = 0.5 \times 10^{-4}$, the error in the estimation of δ due to $\Delta w_c (or \Delta\varphi_D)$ will be $0.5 \times \delta / 10^4$, which is negligible.At this stage of work, MATLAB software is used to conduct 3D simulation. In this simulation, six TXs are assumed to be installed on a hypothetical AOI. So the inputs of MATLAB program are (the locations of) TXs, R_0, and R_1. The location of T' is considered as a reference so that following parameters could be calculated:

- The phase difference between φ_D and φ_D'.
- The estimated angles θ_0, θ_1
- The vector $\vec{M}$ pertaining to 3D vector (matrix) of the slope of the AOI at point T.

It should be mentioned that all simulations are performed on a standard PC with Intel CPU. It is clear that as long as $D - D' < \lambda$ and $\Delta D - \Delta D' = D - D'$, the phase φ_D is much more important than the absolute length of (r_0, r_1). In any case, accurate estimation of vector pertaining to the slope affects the accuracy of calculation of θ_1, θ_0 and consequently δ. In addition, increasing the distance between receivers does not affect δ, but increases the accuracy of calculated $\cos\theta_0 - \cos\theta_1$, $\Delta D - \Delta D'$. Depending on the estimated slope, the error of measurement of θ_1, θ_0 may lead to milder changes in δ (about 6%). As was shown in the above equations, the distance between receivers (α) affects the ambiguous path for each specific TX, and it also affects θ_1, θ_0 and $\Delta D - \Delta D'$. Depending on the wavelength of carrier signal and the location of TX, α should be large enough to maintain the accuracy of calculations by preventing ($\Delta D - \Delta D'$) and ($\cos\theta_0 - \cos\theta_1$) from getting too small. On the other hand, a very large α will have negative effects on the receivers' synchronization clock. In the end, the displacement calculated through this method is compared with the real distance between T and T' obtained from geometrical equations:

$$\mathrm{T_x(x_0, y_0, z_0)} \quad , \mathrm{T_x'(x_1, y_1, z_1)}$$
$$\delta_{\mathrm{Real}} = \sqrt{(\mathrm{x_0 - x_1})^2 + (\mathrm{y_0 - y_1})^2 + (\mathrm{z_0 - z_1})^2} \quad (20)$$

A GUI[1] is designed to simplify the processes of entering coordinates, reviewing the calculations, and plotting simulation results. Details and results of simulation are presented in section 6.

6. RESULTS AND DISCUSSION

To determine the accuracy of proposed method, MATLAB software was used to perform a series of

[1] Graphical User Interface

simulations, where the effects of different states and forms of landslide on an array of six transmitters were evaluated. At the end of this section, we present one instance of these simulations with its related parameters and calculations.

At each step of process, the designed GUI reports the results and their accuracy independently for each transmitter (T1 to T6). This GUI is designed to provide a number of user-friendly features and capabilities, which include:

Component 1: determines the carrier frequency of the system and location of receivers R_0 and R_1.

Component 2: determines the pre-displacement and post-displacement location of first transmitter.

Component 3: determines the pre-displacement and post-displacement location of second transmitter.

Component 4: determines the pre-displacement and post-displacement location of third transmitter.

Component 5: determines the pre-displacement and post-displacement location of fourth transmitter.

Component 6: determines the pre-displacement and post-displacement location of fifth transmitter.

Component 7: determines the pre-displacement and post-displacement location of sixth transmitter.

Component 8: Activates, deactivates, or turns off each transmitter

Component 9: selects a certain transmitter and displays its data.

Component 10: displays the calculated values and the error in calculated δ

Component 11: displays the real-time status of each transmitter

Component 12: displays the status of signals at each step of process

Component 13: displays 3D and 2D representations regarding the status of transmitters and their response to landslide.

Component 14: displays and plots the graphical representations from three perspectives to enhance and simplify the analysis of landslide and its process.

It should be mentioned that user-specified T'_X coordinates are used to calculate the real displacements (δ_{real}) (via the equation of distance between two points in a 3d space) and determine the error of the proposed method.

6.1. Simulation instance

In this section, the following assumptions are used to demonstrate the process and determine the accuracy of proposed approach. The following data are used as the program inputs:

- Carrier frequency (fc): 4 GHz
- Coordinates of the first receiver node (R0): (0,0,0)
- Coordinates of the second receiver node (R1): (1,0,0)
- Coordinates of the first transmitter node (T1): $T_1(10,10,10) \rightarrow T_1'(10.5,10,10)$
- Coordinates of the second transmitter node (T2): $T_2(10,11,10) \rightarrow T_2'(10,11,10.001)$
- Coordinates of the third transmitter node (T3): $T_3(11,10,10) \rightarrow T_3'(11,10,10.001)$
- Coordinates of the fourth transmitter node (T4): $T_4(11,11,10) \rightarrow T_4'(11,11,10.5)$
- Coordinates of the fifth transmitter node (T5): $T_5(12,10,10) \rightarrow T_5'(12,10.1,10)$
- Coordinates of the sixth transmitter node (T6): $T_6(12,11,10) \rightarrow T_6'(12,11.5,10)$

Tables 1, 2, and 3 show the desired parameters and quantities (discussed in section 2.1 and 2.2) obtained from simulation.

Figure 7 shows the GUI window related to the above inputs. This figure displays the input data, calculated parameters (for T_6 for example), received signals (for example $V_{os}(t)$ and $V_{oc}(t)$), and a 3D view of the results. As mentioned earlier, this program can display 3d representations and project them to 2d planes; figure 8 shows these projections on X, Y, and Z planes, which provide a better view for interpretation of results for the occurring of the landslide.

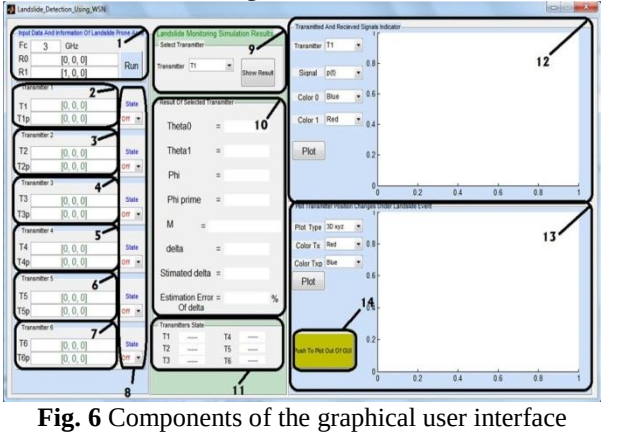

Fig. 6 Components of the graphical user interface (GUI)

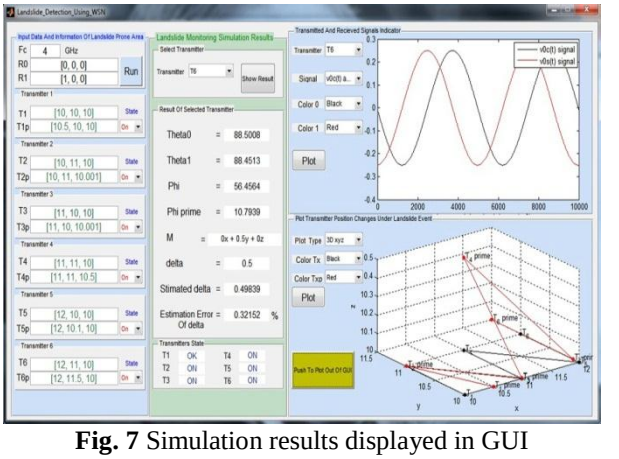

Fig. 7 Simulation results displayed in GUI

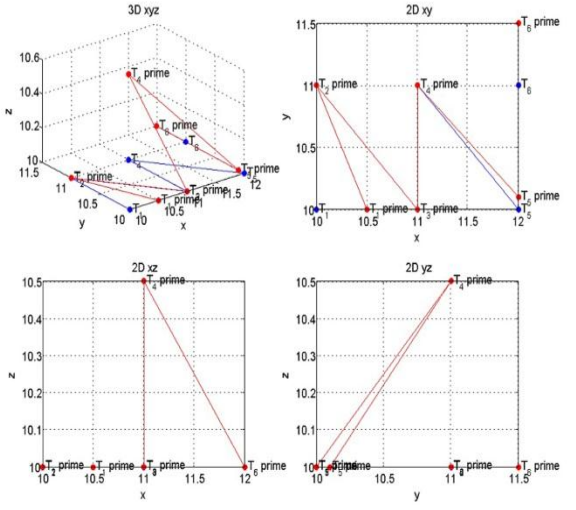

Fig. 8 projections of the simulated post-displacement status on X, Y, and Z planes

Table 1. simulation results obtained for an array of 6 TXs (part1)

φ'_D	φ_D	τ_1	τ_0	r'_1	r'_0	r_1	r_0	Tx
250.6501	155.9104	5.5877e-08	5.7735e-08	17.0367	17.6139	16.7631	17.3205	T1
64.0094	64.0924	5.7927e-08	5.9722e-08	17.3787	17.917	17.3781	17.9165	T2
340.6818	340.774	5.7735e-08	5.9722e-08	17.3211	17.917	17.3205	17.9165	T3
206.7747	248.6303	5.9722e-08	6.1644e-08	18.2003	18.7683	17.9165	18.4932	T4
138.7033	147.8192	5.9722e-08	6.1824e-08	17.9725	18.6013	17.9165	18.5472	T5
10.7939	56.4564	6.1644e-08	6.3683e-08	18.7949	19.3972	18.4932	19.105	T6

Table 2. simulation results obtained for an array of 6 TXs (part2)

D'	Δ_D	D	θ_1	θ_0	M	m_t	m_a	Tx
0.57722	0.032481	0.55745	88.2915	88.3465	0.5x + 0y + 0z	-Inf	1.4524	T1
0.53834	0.013353	0.53833	89.9967	89.9968	0x + 0y + 0.001z	NaN	1.5305	T2
0.59598	0.070995	0.59596	89.9967	89.9968	0x + 0y + 0.001z	NaN	1.3813	T3
0.56808	0.051798	0.57677	88.4014	88.4513	0x + 0y + 0.5z	NaN	1.4487	T4
0.6289	0.030796	0.63076	89.6802	89.6911	0x + 0.1y + 0z	0	1.3255	T5
0.60225	0.011762	0.61173	88.4513	88.5008	0x + 0.5y + 0z	0	1.3841	T6

Table 3. simulation results obtained for an array of 6 TXs (part3)

Estimation error	$\delta_{estimated}$	δ_{real}	$D-D'$	$\Delta_{D'}$	Tx
0.14122%	0.50071	0.5	0.019765	0.052219	T1
4.3305%	0.00055669	0.001	9.6256e-06	0.013335	T2
4.8468%	0.00055153	0.001	1.0593e-05	0.070975	T3
0.33072%	0.49835	0.5	0.0086911	0.043078	T4
1.6607%	0.098339	0.1	0.0018676	0.028897	T5
0.32152%	0.49839	0.5	0.0094824	0.0022487	T6

7. CONCLUSION

In this paper, we introduced a novel method and system for monitoring the displacement in landslide susceptible slopes. In this method, an array of wireless transmitters installed on the AOI broadcast a series of regular signals, which will be received and interpreted by two synchronous receivers. This integrated wireless sensor network gauges the displacements by measuring the phase difference between the two mentioned receivers. The main possible flaw in the principles of this method was defined in the form of an ambiguous path and was addressed in the simulations. We also performed a variety of 3d simulations, where an array of six transmitters was used to monitor displacements in hypothetical landslide susceptible slopes. The proposed system can measure the displacement of each transmitter with a tenth of a millimeter accuracy, and this points to its high potential for landslide monitoring purposes.

REFERENCES

[1] M.-G. Angeli, A. Pasuto, and S. Silvano, "A critical review of landslide monitoring experiences," Engineering Geology, vol. 55, pp. 133-147, 2000.

[2] G. Barrenetxea, F. Ingelrest, G. Schaefer, and M. Vetterli, "The hitchhiker's guide to successful wireless sensor network deployments," in Proceedings of the 6th ACM conference on Embedded network sensor systems, 2008, pp. 43-56.

[3] C. Bonanno, M. Magnani, M. Lapini, and E. Piantelli, "Landslide monitoring system based on integrated automatic total station and gps," Geoitalia, vol. 2, p. 221, 2007.

[4] C. Colesanti and J. Wasowski, "Investigating landslides with space-borne Synthetic Aperture Radar (SAR) interferometry," Engineering geology, vol. 88, pp. 173-199, 2006.

[5] A. P. Dempster, N. M. Laird, and D. B. Rubin, "Maximum likelihood from incomplete data via the EM algorithm," Journal of the royal statistical society. Series B (methodological), pp. 1-38, 1977.

[6] G. Luzi, Ground based SAR interferometry: a novel tool for Geoscience: INTECH Open Access Publisher, 2010.

[7] M. V. Ramesh, "Real-time wireless sensor network for landslide detection," in Sensor Technologies and Applications, 2009. SENSORCOMM'09. Third International Conference on, 2009, pp. 405-409.

[8] M. A. Richards, "A Beginner's Guide to Interferometric SAR Concepts and Signal Processing [AESS Tutorial IV]," Aerospace and Electronic Systems Magazine, IEEE, vol. 22, pp. 5-29, 2007.

[9] T. SAKAI, J. H. JEONG, and M. TAKAGI, "Measurement method of landslide displacement with ground based portable laser scanner," in Proceedings of International Symposium on Management Systems for Disaster Prevention, 2006.

[10] K. Taneda, S. Niimi, and S. Takayama, "Estimation method of dynamic behaviors of network sensing node at landslide disaster," in SICE Annual Conference (SICE), 2011 Proceedings of, 2011, pp. 2019-2023.

[11] B.-C. Wang, Digital signal processing techniques and applications in radar image processing vol. 91: John Wiley & Sons, 2008.
[12] S.Shoorabi Sani, M.Baghaei-Nejad, M.Kalate Aarabi ," Using a phase difference detection technique for monitoring the structural health of bridge piers", STRUCTURAL CONTROL AND HEALTH MONITORING, In Press.
[13] S.Shoorabi Sani, M.Baghaei-Nejad, M.Kalate Aarabi ," Remote Detection of Earthquake Induced Damages on Bridge Piers Using WSN Based on Dual Receiver and Phase Difference Measurement Technique", journal of Siesmology & Earthquake Engineering, In Press.
[14] M.H.Shahrokh abadi , S.Shoorabi sani ," A novel system based on dual-receiver for movement detection in structures : a bridge case study", Int. J. Systems, Control and Communications,In Press.
[15] S.Shoorabi Sani, M.Kalate Arabi , " Application Of Inexpensive Sensors For SHM Of Bridges Improved By Fuzzy Inference And Data Mining Techniques". J. of Active and Passive Electronic Devices , In Press.
[16] S.Shoorabi Sani ," Overcome To Some Technical Limitations And Challenges In Structural Health Monitoring Of Concrete Structures Using Wireless Sensor Networks", J. of Active and Passive Electronic Devices , In Press.
[17] S.Shoorabi Sani , M.Baghaei-Nejad , M.Kalate Arabi ," A New Inexpensive System For SHM Of Bridge Decks Capable Of Issuing Alarms Regarding Bridge Maintenance Using Wireless Sensor Networks Based On Measurements OF Temperature And Humidity", Structural Durability & Health Monitoring ,In Press.